PROCEEDINGS OF SCIENCE

Enhanced Ultra-High Energy Neutrino Search at the Askaryan Radio Array using Template-based Techniques

Myoungchul Kim[a,*] **for the ARA Collaboration**
(a complete list of authors can be found at the end of the proceedings)

[a] *Chiba University, Chiba 263-8522, JAPAN*
E-mail: mkim@icecube.wisc.edu

The Askaryan Radio Array (ARA) is a gigaton-size neutrino radio telescope situated near the geographic South Pole, which has been in operation since 2011. It is specifically designed to detect Askaryan emissions resulting from the interaction between ultra-high energy neutrinos (> 10 PeV) and Antarctic ice. Each of the five ARA stations is equipped with 16 antenna clusters arranged in a cubic configuration, approximately ~200 m deep in the ice. In this analysis, we utilize data from two ARA stations with a total livetime of ~10.5 years, representing a two times increase in exposure time compared to the previous ARA result. To enhance the detection of neutrinos at the ARA, we introduce the template method known as a matched filter, which was inspired by analysis methods used by the Laser Interferometer Gravitational-Wave Observatory (LIGO) Collaboration. This method entails the direct comparison of data with simulated neutrino signal templates, facilitating the identification of low signal-to-noise ratio (SNR) neutrino signatures, ultimately resulting in an improved low energy threshold. Our study presents the diffuse neutrino search results derived from the analysis of data, with an estimated factor of 4 sensitivity improvements above 10 PeV. These improvements were achieved through a factor of 2.3 improvement in analysis efficiency due to the application of the matched filter technique and a factor of 1.7 increase in livetime.

38th International Cosmic Ray Conference (ICRC2023)
26 July - 3 August, 2023
Nagoya, Japan

ICRC2023
38th International Cosmic Ray Conference
The Astroparticle Physics Conference

*Speaker

PoS(ICRC2023)1148

1. Introduction

Ultra-High Energy Cosmic Rays (UHECRs) are believed to originate from cosmic accelerators and have been observed by prominent telescopes such as the Telescope Array (TA) and Pierre Auger Observatory (Auger) [1, 2]. However, the origin of UHECRs remains a mystery. One promising way to understand the acceleration and propagation mechanisms of UHECRs is by detecting ultra-high energy (UHE) neutrinos that result from the interaction between UHECRs and Cosmic Microwave Background (CMB) photons, known as the Greisen-Zatsepin-Kuzmin (GZK) suppression [3, 4]. The cosmogenic or GZK neutrinos produced from this interaction can provide insights into understanding UHECRs, such as their propagation mechanisms and mass composition [5].

Detection of UHE neutrinos has been a significant challenge, primarily due to their low flux [6], expecting an event per 100 gigatons of ice per year for UHE neutrinos. With its large volume and radio transparency, the ice in Antarctica offers an ideal medium for constructing a detector capable of capturing UHE neutrinos.

When UHE neutrinos interact with the Antarctic ice, they produce particle cascades which emits radiation via the Askaryan effect along the Cherenkov cone [7–9]. This creates coherent radio waves when the radiation wavelength is longer than the shower size. In the radio-transparent Antarctic ice, unlike optical light, coherent radio waves do not scatter and can have an attenuation length of ~1 km [10]. Thus, this characteristic allows the Askaryan Radio Array (ARA) to deploy each station, a cluster of antennas, in ~2 km distance with a hexagonal pattern.

In this proceeding, we present the results of the diffuse neutrino search by analyzing the burn sample. Additionally, we estimate the sensitivity of the detector through simulations and corresponding livetime calculations.

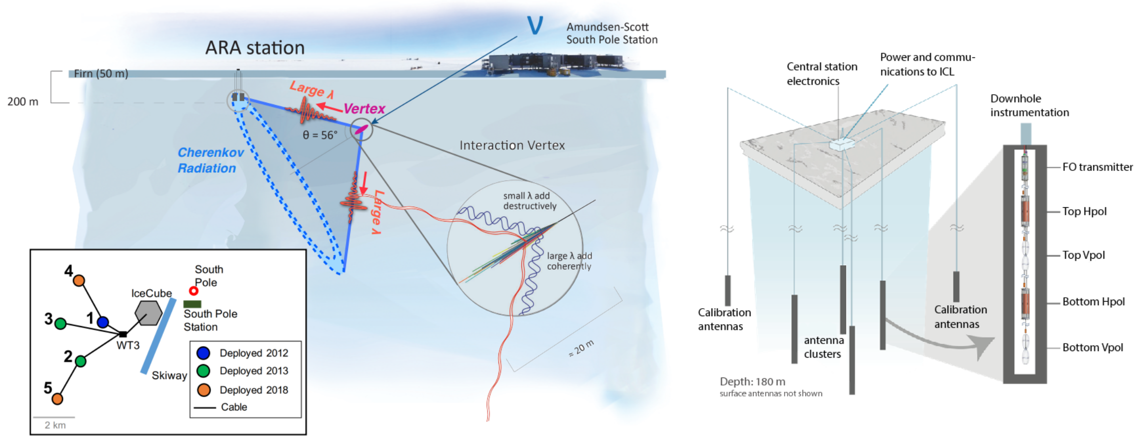

Figure 1: Left: The currently deployed ARA stations layout and a diagram illustrating the Cherenkov radiation produced by the interaction between UHE neutrinos and the Antarctic ice. Right: The schematic of the individual ARA station.

2. ARA Detector

The ARA detector is a neutrino telescope located in the glacial ice near the South Pole. The primary objective of ARA is detecting UHE neutrinos with energies above 10^{16} eV. The ARA detector consists of five autonomous stations deployed up to 200 meters below the Antarctic ice surface.

Each ARA station has 20 radio frequency (RF) antennas and corresponding electronics arranged in six strings below the ice. At the surface of the ice, a data acquisition (DAQ) system is positioned to collect the measured data from the antennas. The 16 antennas are deployed in a cubic configuration, facilitating the observation of neutrino-induced radio signals with precise timing information for vertex reconstruction. Additionally, four antennas are positioned approximately ~40 m away from the center of the 16 antennas. These specific antennas are designed to transmit known pulses, serving the purpose of calibration.

The RF antennas consist of two types: sensitive to vertically-polarized (VPol) signals and sensitive to horizontally-polarized (HPol) signals. It allows for identifying the electric field (E-field) polarization, which is crucial for reconstructing the direction of the neutrinos. The schematic design of the ARA detector is illustrated in Figure 1.

The ARA operates at a ~7 Hz trigger rate. The tunnel diode within the DAQ initiates the readout process when the integrated power of the incoming signal exceeds the thermal noise by roughly five times. The data collected using this trigger algorithm consists of ~6 Hz, encompassing the thermal noise background, anthropogenic signals, and calibration pulses. The software trigger attributes the remaining ~1 Hz.

2.1 Data Samples

This proceeding focuses on data measured from the second and third ARA stations (A2 and A3). Both A2 and A3 started taking data in 2013. The data collected during the period from 2013 to 2020 was utilized for this analysis. The corresponding accumulated livetime of A2 is ~1989 days, and for A3, it is ~1924 days, as shown in Figure 2. The total ~2 billion events were recorded from the two stations. The total data is categorized into five configurations for A2 and nine configurations for A3, as the detector parameters were optimized, including the number of active antennas and readout window sizes.

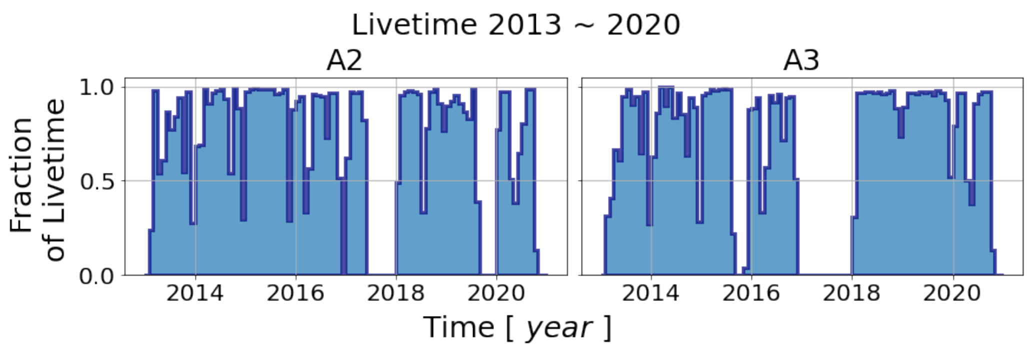

Figure 2: The fraction of live time for A2 and A3 during the 2013 to 2020 period. A2 has ~1989 days of accumulated live time, and A3 has ~1924 days of accumulated live time.

3. Simulation

The expected neutrino-induced signal that ARA can observe is simulated using AraSim [11]. This simulation includes the Askaryan radiation model [8], which considers the neutrino-induced signal propagation in the ice. Additionally, the South Pole ice model incorporates characteristics of the depth-dependent index of refraction.

In this proceeding, we utilized the realistic detector model by incorporating data measured by software trigger, representing internal detector noise [12]. With this model, we generated the thermal noise background expected from the ice at the South Pole.

The simulated neutrino events are randomly distributed within the spherical trigger volume with a ∼12 km radius, where the simulated ARA stations are located at the center. The events are generated based on a power law spectrum with a flux proportional to E^{-1} from 10^{16} eV to 10^{21} eV.

In this analysis, we individually simulated each station data configurations to accurately model detector optimization by incorporating their parameters. Figure 3 shows each stations trigger level effective area, obtained by averaging all the configurations.

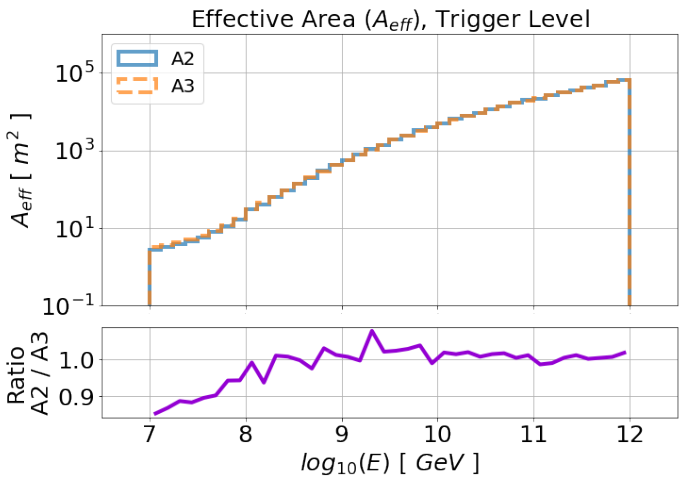

Figure 3: Top: The simulated trigger-level effective area for A2 and A3. Bottom: Ratio of the effective areas for A2 and A3

4. Data Analysis

This analysis aims to search for potential neutrino signatures present in the ARA data. It excludes known background sources, such as thermal and anthropogenic noise, while isolating neutrino-induced events. The analysis is conducted in a blinded technique, only using 10% of the randomly selected data (burn sample) to minimize bias toward the data and ensure the integrity of the results. Using this burn sample, We developed quality cuts to remove known background sources systematically. Due to the absence of neutrino signatures in the burn sample, we estimated the sensitivity of the detector by using simulation results, assuming the analysis of 100% data. In the near future, we will apply this analysis technique to the entire dataset to search for neutrino events.

4.1 The Matched Filter Technique

We introduced the matched filter (MF) technique, inspired by LIGO, into our ARA data analysis as one of the main parameters for the signal-background separation [12–14]. This technique is designed to identify the desired signal from the dominant stochastic noise waveforms by directly cross-correlating the modeled signal as a template.

The neutrino template sets are generated by AraSim. We considered four parameters for constructing template sets: the realistic detector model estimated from the data, the zenith angle-dependent antenna gain pattern, the energy contribution from both the electromagnetic (EM) and hadronic (HAD) shower models, and whether the signal is on- or off-cone based on the Askaryan effect [15]. These parameters play a crucial role in controlling the signal waveform shape. Other parameters, such as neutrino energy and the distance from the vertex to the detector, can be simplified using a scale factor.

We analyzed all the events from the data and the simulated neutrino signal using the MF technique. The cross-correlation results as a function of the lag time, including the Hilbert envelope $M(t)$ can be expressed like,

$$M(t) = \int_0^\infty \frac{D(f)T^*(f)}{P(f)} e^{2\pi i f t} df \tag{1}$$

where $D(f)$ is a frequency spectrum of the data, $T^*(f)$ represents a frequency spectrum of the time-reversed template, and $P(f)$ is the power spectral density (PSD) of thermal noise. And we also obtained a normalization factor σ for normalizing the power of $T(f)$ and $P(f)$. The σ can be described by

$$\sigma^2 = \int_0^\infty \frac{|T(f)|^2}{P(f)} df \tag{2}$$

After obtaining $M(t)$ and σ from the individual channel, we merged the results based on the same-polarization type to amplify the neutrino signature. During this merging process, the arrival time delay estimated from the ray-tracing algorithm in AraSim is removed. This merged MF $M_{sum}(t)$ is given by

$$M_{sum}(t) = \sqrt{\frac{\sum_1^n \mathrm{M}_n(t+\tau_n)}{\sum_1^n \sigma_n^2}} \tag{3}$$

Where n is the number of channels and τ_n is the arrival time delay based on the ray-tracing [12, 13]. The event-wise MF values, $M_{\max}$, is given by the maximum value of $M_{sum}(t)$. The $M_{\max}$ from each polarization is utilized for the data analysis.

4.2 Background Rejection

Systematic background removal mainly targets noise from DAQ glitches and anthropogenic (human-made) noise.

The first level of the background rejection corresponds to events contaminated by noise coming from DAQ glitches. We removed these events by cross-checking secondary information, such as the amount of voltage that goes into the digitizer board in the DAQ. We also applied a band-pass filter for outside of the RF frequency range for 130-850 MHz to suppress excess power produced by DAQ glitches.

From December 2018 to December 2019, an ARA digitizer board experienced dead-bit issues causing events with missing data. This issue has been fixed, but data taken from that specific period has been excluded from the analysis.

The second level corresponds to removing anthropogenic noise. One of the consistent backgrounds in this category is the continuous wave (CW) events from weather balloon communication signatures. These events occur twice daily at the South Pole, and during the weather balloon flights, ARA observes their communication signal at frequencies of ~410 MHz in the data. To filter out this contamination signal from data, we applied the geometric method, as implemented by the ANITA Collaboration [16].

Other sources of anthropogenic noise include mistagged calibration pulse events that may have leaked into the data. To exclude these signals, we developed a cut using the interferometric technique, which is designed to reconstruct the position of the source [17]. The mistagged calibration pulse events are removed using a geometric cut. First, we estimated the position of the reconstructed calibration pulse regions based on known calibration pulse events. Then, any event with a reconstructed position within that region is excluded from the analysis.

The final anthropogenic source is surface activity at the South Pole. These events are expected to be produced above the surface and have an impulsive shape compared to thermal noise. We excluded these events using the interferometric and MF technique. If the reconstructed zenith angle by either technique is smaller than 55 °, it is removed from the analysis. The simulated neutrino templates used in the MF technique are also categorized based on different zenith angles due to antenna angular gain differences. Due to the impulsive nature of the noise, the MF technique was also able to reconstruct its zenith angle.

We applied this systematic background removal to data from each configuration of both stations. This results in live time losses of ~12 % for A2 and ~11 % for A3 at the data. We also applied the same cuts on the simulation to calculate losses of signal efficiencies. We expect an average ~30 % of signal efficiency losses from both stations. These losses are mainly from the cut designed to remove surface activity. We are currently in the process of fine-tuning this surface-cut threshold.

4.3 Results

After going through all the background rejection steps, we expected the remaining data to consist of thermal noise events or potential neutrino candidates. At this step, We utilized the interferometric and MF techniques to remove dominant thermal noise from possible neutrinos. The interferometric technique has a strong advantage in finding similarities between data, while the MF technique is optimized to find hidden signals from data by directly comparing them to the simulated neutrino signal as a template. We developed the final cut by making the diagonal fit in the 2d plane based on two parameters, as shown in Figure 4. The simulation is re-weighted by the neutrino flux model of [5]. Due to the significant challenge of establishing the detector noise model by simulation, this signal-background separation is performed with a data-driven model. In this proceeding, We could not estimate the uncertainty of background estimation and systematic uncertainties of the detector. These uncertainties will be evaluated in the future. Additionally, this analysis does not consider coincident events between A2 and A3, which are expected to be negligible. A detailed study about observing coincident events by all ARA stations is presented in [18]

We did not find any neutrino candidates from the burn samples. However, as the final optimization of this analysis is still in progress, we expect to apply more fine-tuned cuts on the full dataset in the future. We estimated preliminary sensitivity based on the burn sample analysis, as shown in Figure 5. The signal efficiencies are estimated using the simulated neutrino events that passed all the cuts. When merging the results from each station and configuration, we also applied the corresponding live time to obtain the global sensitivity of the detector. Based on the estimated sensitivity, we anticipate an improvement compared to the previous analysis by a factor of ~4. These improvements were attained through a factor of ~1.7 increase in livetime and a factor of ~2.3 improvement in analysis efficiency. Based on this analysis, we would expect to observe a total of ~0.2 events from the combined livetime of A2 and A3 based on the flux model of [5].

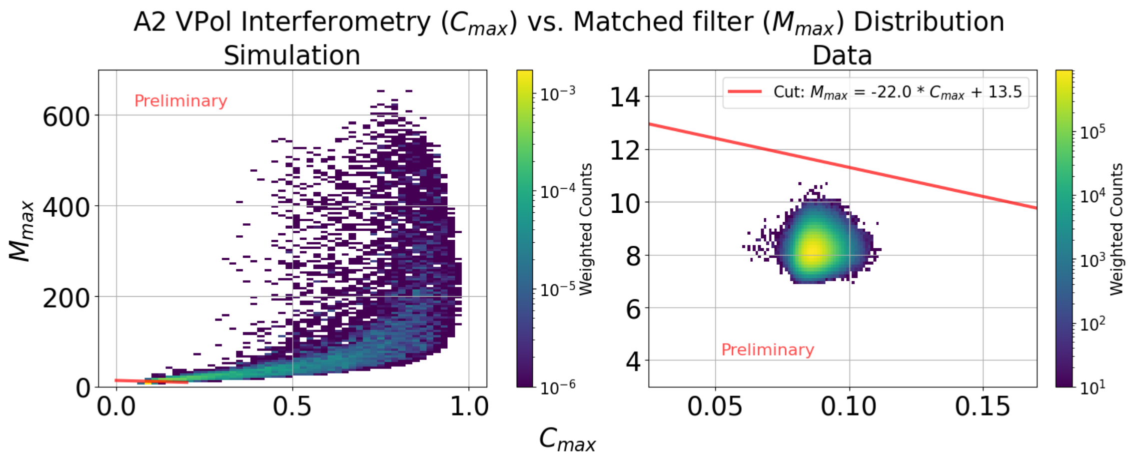

Figure 4: An example of the 2d cut plane consists of interferometric and MF parameters by VPol data from A2 first configuration. Left: The distribution made by simulated neutrino signal. Right: The distribution from ARA data.

5. Conclusion

We have presented the results of the diffuse neutrino search using data measured by the ARA, focusing on the A2 and A3 stations. The continuous measurement by the ARA detector and implementation of MF technique demonstrated improvement in the search for UHE neutrino signal. While no neutrino candidates were found in the burn samples, ongoing analysis optimization is promising to improve the search in the 100% dataset.

Additionally, the ARA Collaboration aims to perform a combined analysis that incorporates all five ARA stations and the phased array [19]. With an accumulated 24 station-years amount of dataset, ARA holds significant potential for making new discoveries in the future.

References

[1] **Telescope Array** Collaboration, P. Tinyakov *Nucl. Instrum. Meth. A* **742** (2014) 29–34.

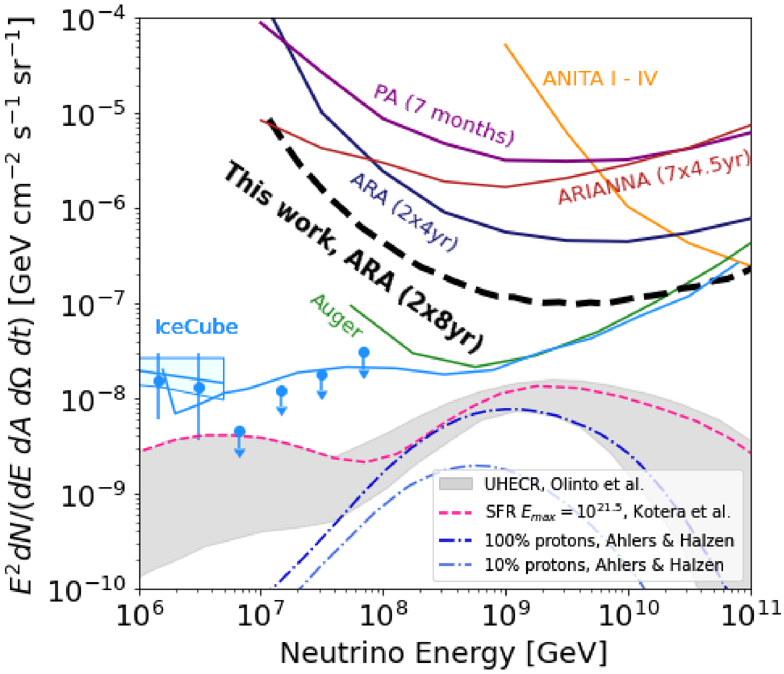

Figure 5: The 90 % CL upper limit on the diffuse neutrino flux by A2 and A3 analysis (black dashed line).

[2] **The Pierre Auger** Collaboration *The Astrophysical Journal* **802** no. 2, (Mar, 2015) 111.

[3] K. Greisen *Phys. Rev. Lett.* **16** (1966) 748–750.

[4] G. T. Zatsepin and V. A. Kuzmin *JETP Lett.* **4** (1966) 78–80.

[5] K. Kotera, D. Allard, and A. Olinto *Journal of Cosmology and Astroparticle Physics* **2010** no. 10, (Oct, 2010) 013.

[6] A. Connolly, R. S. Thorne, and D. Waters *Phys. Rev. D* **83** (2011) 113009.

[7] M. Ahlers and F. Halzen *Phys. Rev. D* **86** (Oct, 2012) 083010.

[8] J. Alvarez-Muñiz and E. Zas *Physics Letters B* **411** no. 1, (1997) 218–224.

[9] G. A. Askar'yan *Zh. Eksp. Teor. Fiz.* **41** (1961) 616–618.

[10] **ARA** Collaboration, P. Allison *et al.* *Astroparticle Physics* **35** no. 7, (Feb., 2012) 457–477.

[11] **ARA** Collaboration, P. Allison *et al.* *Astropart. Phys.* **70** (2015) 62–80.

[12] **ARA** Collaboration, M. Kim *et al.* *PoS* **ICRC** (2021) 1147.

[13] **LIGO Scientific** Collaboration *Phys. Rev. D* **69** (Jun, 2004) 122001.

[14] L. Wainstein, V. D. Zubakov, and A. A. Mullin, "Extraction of signals from noise," 1970.

[15] P. Allison *et al.* *Nucl. Instrum. Meth. A* **930** (2019) 112–125.

[16] **ANITA** Collaboration, P. W. Gorham *et al.* *Phys. Rev. D* **98** no. 2, (2018) 022001.

[17] **ARA** Collaboration, P. Allison *et al.* *Phys. Rev. D* **102** no. 4, (2020) 043021.

[18] **ARA** Collaboration, A. Bishop *et al.* *PoS* **ICRC** (2023) 1169.

[19] **ARA** Collaboration, P. Dasgupta, M. S. Muzio, *et al.* *PoS* **ICRC** (2023) 1226.

Full Author List: ARA Collaboration (July 18, 2023)

S. Ali[1], P. Allison[2], S. Archambault[3], J.J. Beatty[2], D.Z. Besson[1], A. Bishop[4], P. Chen[5], Y.C. Chen[5], B.A. Clark[6], W. Clay[7], A. Connolly[2], K. Couberly[1], L. Cremonesi[8], A. Cummings[9,10,11], P. Dasgupta[12], R. Debolt[2], S. de Kockere[13], K.D. de Vries[13], C. Deaconu[7], M. A. DuVernois[4], J. Flaherty[2], E. Friedman[6], R. Gaior[3], P. Giri[14], J. Hanson[15], N. Harty[16], B. Hendricks[9,10], K.D. Hoffman[6], J.J. Huang[5], M.-H. Huang[5,17], K. Hughes[9,10,11], A. Ishihara[3], A. Karle[4], J.L. Kelley[4], K.-C. Kim[6], M.-C. Kim[3], I. Kravchenko[14], R. Krebs[9,10], C.Y. Kuo[5], K. Kurusu[3], U.A. Latif[13], C.H. Liu[14], T.C. Liu[5,18], W. Luszczak[2], K. Mase[3], M.S. Muzio[9,10,11], J. Nam[5], R.J. Nichol[8], A. Novikov[16], A. Nozdrina[1], E. Oberla[7], Y. Pan[16], C. Pfendner[19], N. Punsuebsay[16], J. Roth[16], A. Salcedo-Gomez[2], D. Seckel[16], M.F.H. Seikh[1], Y.-S. Shiao[5,20], D. Smith[7], S. Toscano[12], J. Torres[2], J. Touart[6], N. van Eijndhoven[13], G.S. Varner[21], A. Vieregg[7], M.-Z. Wang[5], S.-H. Wang[5], S.A. Wissel[9,10,11], C. Xie[8], S. Yoshida[3], R. Young[1]

[1] Dept. of Physics and Astronomy, University of Kansas, Lawrence, KS 66045
[2] Dept. of Physics, Center for Cosmology and AstroParticle Physics, The Ohio State University, Columbus, OH 43210
[3] Dept. of Physics, Chiba University, Chiba, Japan
[4] Dept. of Physics, University of Wisconsin-Madison, Madison, WI 53706
[5] Dept. of Physics, Grad. Inst. of Astrophys., Leung Center for Cosmology and Particle Astrophysics, National Taiwan University, Taipei, Taiwan
[6] Dept. of Physics, University of Maryland, College Park, MD 20742
[7] Dept. of Physics, Enrico Fermi Institue, Kavli Institute for Cosmological Physics, University of Chicago, Chicago, IL 60637
[8] Dept. of Physics and Astronomy, University College London, London, United Kingdom
[9] Center for Multi-Messenger Astrophysics, Institute for Gravitation and the Cosmos, Pennsylvania State University, University Park, PA 16802
[10] Dept. of Physics, Pennsylvania State University, University Park, PA 16802
[11] Dept. of Astronomy and Astrophysics, Pennsylvania State University, University Park, PA 16802
[12] Université Libre de Bruxelles, Science Faculty CP230, B-1050 Brussels, Belgium
[13] Vrije Universiteit Brussel, Brussels, Belgium
[14] Dept. of Physics and Astronomy, University of Nebraska, Lincoln, Nebraska 68588
[15] Dept. Physics and Astronomy, Whittier College, Whittier, CA 90602
[16] Dept. of Physics, University of Delaware, Newark, DE 19716
[17] Dept. of Energy Engineering, National United University, Miaoli, Taiwan
[18] Dept. of Applied Physics, National Pingtung University, Pingtung City, Pingtung County 900393, Taiwan
[19] Dept. of Physics and Astronomy, Denison University, Granville, Ohio 43023
[20] National Nano Device Laboratories, Hsinchu 300, Taiwan
[21] Dept. of Physics and Astronomy, University of Hawaii, Manoa, HI 96822

Acknowledgements

The ARA Collaboration is grateful to support from the National Science Foundation through Award 2013134. The ARA Collaboration designed, constructed, and now operates the ARA detectors. We would like to thank IceCube and specifically the winterovers for the support in operating the detector. Data processing and calibration, Monte Carlo simulations of the detector and of theoretical models and data analyses were performed by a large number of collaboration members, who also discussed and approved the scientific results presented here. We are thankful to the Raytheon Polar Services Corporation, Lockheed Martin, and the Antarctic Support Contractor for field support and enabling our work on the harshest continent. We are thankful to the National Science Foundation (NSF) Office of Polar Programs and Physics Division for funding support. We further thank the Taiwan National Science Councils Vanguard Program NSC 92-2628-M-002-09 and the Belgian F.R.S.- FNRS Grant 4.4508.01 and FWO. K. Hughes thanks the NSF for support through the Graduate Research Fellowship Program Award DGE-1746045. B. A. Clark thanks the NSF for support through the Astronomy and Astrophysics Postdoctoral Fellowship under Award 1903885, as well as the Institute for Cyber-Enabled Research at Michigan State University. A. Connolly thanks the NSF for Award 1806923 and 2209588, and also acknowledges the Ohio Supercomputer Center. S. A. Wissel thanks the NSF for support through CAREER Award 2033500. A. Vieregg thanks the Sloan Foundation and the Research Corporation for Science Advancement, the Research Computing Center and the Kavli Institute for Cosmological Physics at the University of Chicago for the resources they provided. R. Nichol thanks the Leverhulme Trust for their support. K.D. de Vries is supported by European Research Council under the European Unions Horizon research and innovation program (grant agreement 763 No 805486). D. Besson, I. Kravchenko, and D. Seckel thank the NSF for support through the IceCube EPSCoR Initiative (Award ID 2019597). M.S. Muzio thanks the NSF for support through the MPS-ASCEND Postdoctoral Fellowship under Award 2138121.